Hole and electron traps in the $YAlO_3$ single crystal scintillator

V. V. Laguta,[1] M. Nikl,[1] A. Vedda,[2] E. Mihokova,[1,2] J. Rosa,[1] and K. Blazek[3]
[1]*Institute of Physics, Academy of Sciences of the Czech Republic, 10 Cukrovarnická Street, 16253 Prague 6, Czech Republic*
[2]*Department of Materials Science, University of Milano–Bicocca, via Cozzi 53, 20125 Milan, Italy*
[3]*CRYTUR Ltd., Palackeho 175, 511 19 Turnov, Czech Republic*
(Received 14 January 2009; revised manuscript received 5 June 2009; published 16 July 2009)

The processes of hole and electron localization in $YAlO_3$ single crystals were investigated by electron-spin resonance. It was found that holes created by UV or x-ray irradiation are trapped at regular oxygen ions forming two types of O^- hole centers corresponding to hole localization at two inequivalent oxygen ions which are located in Y and Al planes, respectively. The hole can be either autolocalized or additionally stabilized by a defect in the neighborhood of the oxygen ion such as yttrium vacancy or an impurity ion at Y site. This leads to a variety of O^- centers which differ both by thermal stability (from about 14 K up to room temperature) and spectral parameters. Electron-type trapping sites are assigned to Y_{Al} antisite ions. After trapping an electron they become paramagnetic Y_{Al}^{2+} centers. They are found in several configurations with thermal stability up to above 300 K that enables the radiative recombination of freed holes with such localized electrons and the appearance of thermoluminescence peaks. It is shown that the electron trapped around Y_{Al} antisite ion is additionally stabilized either by an oxygen vacancy or by a defect at Y site. The yttrium antisite ions in the lattice were directly identified by ^{89}Y nuclear magnetic resonance.

DOI: 10.1103/PhysRevB.80.045114 PACS number(s): 61.72.−y, 76.30.Mi, 61.82.Ms, 71.38.Ht

I. INTRODUCTION

A scintillating material is a converter transforming the energy of photons of ionizing radiation (x or γ rays) or accelerated particles (protons, electrons, neutrons, α particles, etc.) into a number of UV/visible photons easily detectable with a conventional photomultiplier or semiconductor diode. Wide band-gap insulator materials of high degree of structural perfection are the most suitable scintillating materials. They found applications in many fields, e.g., in industrial defectoscopy, modern medical-imaging methods, security systems, detectors in high energy, and nuclear physics.[1] In particular, Ce-doped Y-Al perovskite ($YAlO_3$, commonly denoted as YAP) bulk single crystals have already been recognized a time ago as high figure-of-merit scintillators.[2] Apart from the best performing Ce^{3+} doped also the Yb^{3+}- and Pr^{3+}-doped YAP single crystals have been studied to develop faster-than-Ce^{3+} scintillating materials.[3–6] However, due to the high-growth temperatures of YAP single crystals, the existence of complex cation sublattices and the presence of cations of equal charge state in various lattice sites, a variety of point defects can occur. Among them, vacancies and the so-called antisite defects (i.e., Y at the Al site and vice versa) as well as their aggregates with other defects and impurities are of particular importance.[7,8] Anion and cation vacancies can often create parent sites for electron and hole capture, respectively,[9–12] and such traps can easily degrade both the light yield and time characteristics of a scintillator. Antisite defects can induce shallow trap levels in the forbidden gap as it follows from the theoretical calculations.[13,14] The presence of Ce^{3+} at Al^{3+} site was proposed to explain the luminescence properties of YAP:Ce.[15] The presence of the antisite defects is an inevitable consequence of the high-growth temperature (about 2000 °C) of the bulk crystals grown from the melt by Czochralski, Bridgman, or similar methods. It is worth noting that scintillation decay of YAP crystals shows a noticeable presence of slow components originating from delayed radiative recombination of electrons and holes at Ce^{3+} centers, most probably caused by their retrapping at shallow traps during the transport stage.[9,16,17] Even deeper traps reported in YAP:Ce can be responsible for the induced absorption phenomena at RT usually referred to as radiation damage resulting in gradual decrease in light yield due to reabsorption losses.[10,18]

The above brief survey indicates that the intermediate transport stage of the scintillation mechanism is a substantially critical and yet poorly predictable part of the process since any kind of trapping levels in the forbidden gap and/or nonradiative recombination centers can significantly decrease the scintillator performance. It should be stressed, however, that optical characterization (radiation-induced absorption and thermally stimulated luminescence) clearly demonstrates the presence of a variety of trapping centers in variously doped YAP single crystals (see, e.g., Refs. 6, 10, and 18–20). Nevertheless, their nature in most of the cases has so far been only partly understood.

Experimental efforts aimed at understanding the nature of defects in YAP crystals involved thermally stimulated luminescence (TSL) and electron-spin-resonance (ESR) studies. Especially, ESR and related magnetic-resonance methods can provide valuable information on the nature and local structure of trapping centers/defects. In a pioneering work of Schirmer *et al.*,[21] ESR after UV or visible irradiation of YAP evidenced a localization of holes in the form of O^- bound small polarons. Recently we found up to five different O^- center configurations, three of which were correlated with TSL peaks observed below room temperature.[22,23] Electron-type traps/defects were also detected in UV irradiated YAP crystals[23] and it was preliminary suggested that they can be attributed to the charged oxygen vacancy near the antisite yttrium ion, i.e., F^+ centers could be created. Therefore, TSL recombination could occur between holes thermally freed from O^- centers and electrons trapped at oxygen vacancies.

Such mechanism takes place in crystals that are pure or slightly doped by Ce. In a heavily Ce-doped sample the TSL glow curve is characterized by one or two dominant peaks at 110–150 K, with an athermal tunneling emission at its lower-temperature side.[24]

In this paper we continue to investigate the intrinsic hole and electron traps in yttrium aluminum perovskite by electron-spin resonance. In particular, we want to clarify their local structure, to determine thermal-stability parameters, and to clarify their role in the energy transfer and storage processes of YAP scintillator. Some of the preliminary results related to the defects studied here have been briefly reported previously.[23]

II. EXPERIMENTAL CONDITIONS

Single crystals of undoped and weakly Ce-doped Y-Al perovskites (Ce concentration in the crystals 0.005 at. %) were grown by the Czochralski technique from 6N Y_2O_3 and 4N Al_2O_3 (undoped), 5N Y_2O_3 and 4N Al_2O_3, and 4N CeO_2 (the Ce-doped samples) raw powders in a molybdenum crucible under reducing atmosphere by CRYTUR Ltd. (Turnov, Czech Republic); see Ref. 25 for more details about the growth procedure. YAP crystallizes in a slightly distorted perovskite structure. It is characterized by the space group $D_{2h}^{16}(Pbnm)$ with the unit-cell dimensions $a=5.180$ Å, $b=5.330$ Å, and $c=7.375$ Å. The orthorhombic unit cell contains four perovskite pseudocells. The main crystallographic parameters of YAP can be found, e.g., in Ref. 26 or in Ref. 21.

For ESR measurements, the crystals were oriented, polished, and cut in the (100), (010), and (001) planes in a typical shape of about $2\times2.5\times6$ mm^3. The same crystals were also used in the TSL measurements.[22,27] ESR measurements were performed at 9.22 GHz with the standard 3 cm wavelength of the ESR spectrometer in the temperature range 10–260 K using an Oxford Instruments cryostat. A mercury high-pressure arc lamp with optical filters was used for *in situ* UV irradiation of the samples. Some of the measurements were performed following *in situ* x-ray irradiation. Nuclear magnetic-resonance spectra (NMR) of ^{89}Y and ^{27}Al were measured in a magnetic field $B=9.4$ T, corresponding to a Larmor frequency 19.607 and 104.264 MHz for ^{89}Y and ^{27}Al, respectively. Both single pulse and solid-echo pulse sequences with phase cycling were used. Due to the long spin-lattice relaxation time the repetition time between pulses for yttrium was about 45 min.

III. EXPERIMENTAL RESULTS AND DISCUSSION

In the first subsection we present the ESR characteristics of the hole traps and the data on their thermal stability. Based on these studies, the local structure and creation mechanism of hole centers is considered. In the next subsection we describe electron centers and, in particular, defects related to antisite ions. In the final subsection, electron-hole recombination mechanisms are considered and the role of irradiation-induced centers in scintillation mechanism in YAP:Ce is discussed.

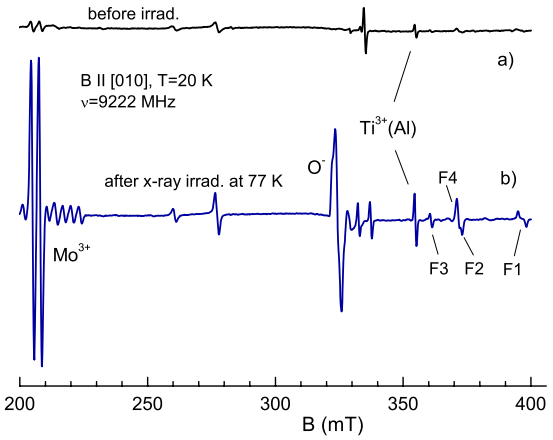

FIG. 1. (Color online) ESR spectra of undoped YAP crystals (a) before and (b) after x-ray irradiation at 77 K.

A. O$^-$ hole centers

1. Spectroscopic data

ESR spectra of YAP crystals before any irradiation show the presence of several types of paramagnetic ions, the most important of which are Mo^{3+} and Ti^{3+} (identified in Refs. 28–30) as they are sensitive to the light or x-ray irradiation of the crystal (Fig. 1). After x-ray irradiation at low temperatures (10–77 K) other intense ESR spectra appear. The intensity of the Mo^{3+} and Ti^{3+} spectra increases. The same transformation of the spectra can also be produced by UV (280–365 nm) light illumination. Therefore, most of the experiments were performed using the UV irradiation.

The most intense spectra arise at the magnetic field ~325 mT and belong to O$^-$ ($2p^5$) hole centers in accordance with Ref. 21 and our preliminary study.[22] The spectra at the magnetic fields 360–400 mT, labeled as F1 to F4, were preliminarily assigned by us to the trapped electron centers.[23]

When an irradiated sample is gradually heated from 10 K up to RT, at least six types of O$^-$ centers with different temperature stability and spectral parameters can be distinguished (Fig. 2). The most stable center survives at room temperature for several days while the shallowest one is stable only up to about 14 K. In the following we denote the hole centers as O_I and O_{II} with different upper indexes. The reason of such notation will be understood later. Keeping the sample at RT in the dark for a long time we can restore the initial state of the sample before irradiation. All the O$^-$ spectra show the same pronounced hyperfine structure. The observed splitting into 11 lines is clearly due to the interaction of the electron spin with two equivalent ^{27}Al nuclei ($I=5/2$ and 100% abundance). In the YAP lattice only the spins at the O sites interact with the two adjacent Al nuclei nearly equivalent. Together with positive g factor shifts, all these facts indicate that the paramagnetic substance is a hole trapped at an oxygen ion.

Angular dependencies of O$^-$ resonance lines were measured in three perpendicular planes, (100), (010), and (001). Full sets of the spectroscopic parameters determined from the fits of these angular dependencies are listed in Table I. Spectral parameters of the O_{II}^A center were determined only

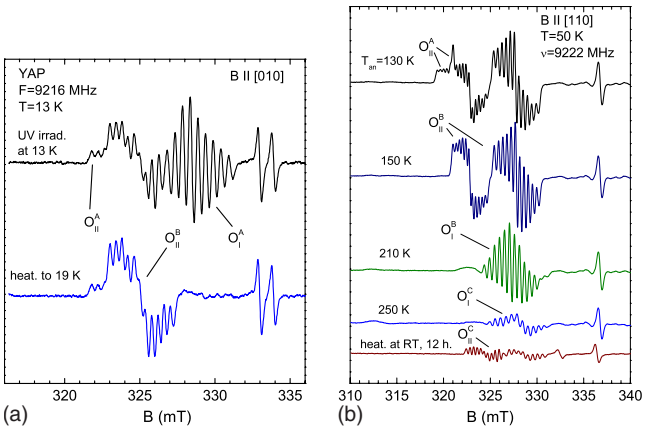

FIG. 2. (Color online) ESR spectra of various O^- centers created in YAP by UV irradiation at 13 K and followed by heating to a given temperature. The spectrum of the shallowest O_I^A center (a) was measured at 13 K with very low MW power, about 1 μW, to overcome saturation of the ESR signal at low temperature. The spectra of other centers (b) were measured at 50 K with MW power of 1 mW. This figure also illustrates transformation of one O^- center into another.

for two separated directions ($\langle 110\rangle$ and $\langle 010\rangle$) because of overlap of its spectral lines with much stronger lines from the O_{II}^B center (Fig. 2). Note that g-tensor parameters of two O^- centers observed previously in Ref. 21 are very close to those of our O_I^B and O_{II}^A centers.

One can see that all centers show an orthorhombic symmetry. They can be divided into two groups: O_I and O_{II}. O_I-type centers have principal axes that exactly coincide with crystal axes or are close to them; the principal axes of O_{II}-type centers are rotated by approximately 45° relative to the crystal axes. For each of the O_{II}-type defects there are two equivalent centers differing only by orientation of their principal axes. These facts indicate that O_I and O_{II} centers correspond to oxygen ions located in the Y and Al planes, respectively, as it is schematically shown in Fig. 3. The figure represents positions of two types of O^- ions in the lattice together with their g-tensor principal-axis orientations. For simplicity, all bond angles were set to 90° (for detailed information on the slightly distorted perovskite structure of YAP see Ref. 26).

A common feature of all O^- centers is that the axis of the largest g-tensor component (g_3) is oriented along Al-O-Al-O… chains. In the case of O_I-type centers this principal axis exactly coincides with the c-crystal direction. The g_3 axis of O_{II}-type centers is rotated from the Al-O-Al-O… direction by about 8° with respect to the a or b axis because of the influence of the rhombic-symmetry distortion of the perovskite lattice in the ab plane. The deviation of the other two g-tensor components from the free-electron value 2.0023 is relatively small. Therefore, in our opinion, the hole is lo-

TABLE I. Characteristics of hole traps in $YAlO_3$ crystals obtained from the ESR data. Principal axes of g tensors are given by polar (θ) and azimuthal (φ) angles relative to the crystal axes a, b, c. Error margin of the polar and azimuthal angles is approximately 2°. O_I and O_{II} correspond to the oxygen ions placed in the Y and Al planes, respectively. The principal-axis directions are given for two equivalent positions of the O_{II}-type centers. All spectral parameters of the O_{II}^A center could not be determined because of overlapping of its spectral lines with much stronger lines from the O_{II}^B center.

Center	g tensor	Principal axes		^{27}Al HF interaction (10^{-4} cm^{-1})	Thermal stability parameters
		θ	φ		
O_I^A	g_1:2.0190(3)	90	22	A_1:4.77(2)	14 K[a]
	g_2:2.0048(3)	90	112	A_2:4.78(2)	$E_a=0.024\pm0.004$ eV
	g_3:2.0344(3)	0	0	A_3:3.83(3)	$s=(2.0\pm0.6)\times10^5$ 1/s
O_{II}^A	$g_{[110]}$:2.054(2)	Not		$A_{[110]}$:3.25(2)	140 K[a]
	$g_{[010]}$:2.035(2)	determined		$A_{[010]}$:3.61(2)	$E_a=(0.40\pm0.02)$ eV
					$s=(3.0\pm1)\times10^{11}$ 1/s
O_{II}^B	g_1:2.0147(2)	134; 46	318; 42	A_1:3.76(2)	185 K[a]
	g_2:2.0034(2)	44; 44	317; 223	A_2:4.11(2)	$E_a=0.49\pm0.04$ eV
	g_3:2.0414(2)	90; 90	47; 133	A_3:3.24(2)	$s=(1.3\pm1)\times10^{11}$ 1/s
O_I^B	g_1:2.0164(2)	90	14	A_1:4.99(2)	240 K[a]
	g_2:2.0045(2)	90	104	A_2:5.05(2)	$E_a=0.48\pm0.05$ eV
	g_3:2.0311(2)	0	0	A_3:4.08(2)	$s=(1.5\pm1)\times10^8$ 1/s
O_I^C	g_1:2.0028(4)	90	0	A_1:4.86(3)	290 K[a]
	g_2:2.0143(4)	90	90	A_2:5.08(4)	(~2–3 h.)
	g_3:2.0440(4)	0	0	A_3:4.29(3)	
O_{II}^C	g_1:2.0117(4)	132; 42	318; 42	A_1:4.23(4)	>300 K[a]
	g_2:2.0043(4)	42; 42	317; 223	A_2:4.23(4)	
	g_3:2.0305(4)	90; 90	47; 133	A_3:3.60(4)	

[a]Temperature of the thermal stability, see Fig. 4.

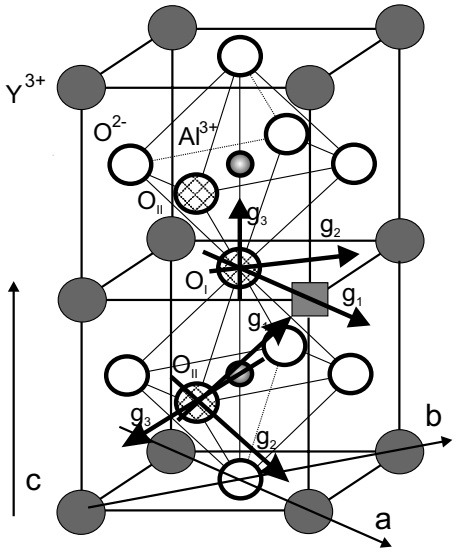

FIG. 3. Idealized fragment of YAP crystal structure (see Ref. 21) with the models of O_I- and O_{II}-type hole centers. All bond angles have been taken to be 90°. A perturbing defect is located at an Y site along the g_1 axis. A hole can be localized in the neighborhood of each type of defect either at an O_I position or at one of the two equivalent O_{II} positions.

calized in all cases in an O $2p_\pi$-type orbital in the plane perpendicular to the Al-O-Al direction. This corresponds to the σ character of O^{2-}-Al^{3+} bonding in the perovskite structure.[13] It should be noted that while for O_{II}-type centers these $2p_\pi$ orbitals are well fixed relative to the crystal axes, i.e., their orientation remains the same for different centers, in case of O_I-type centers the oxygen p_π orbitals are more "mobile" and their rotation with respect to crystal axes increases with the decreasing thermal stability of the center. Consequently, the principal-axis frame of the shallowest center is rotated by 22^0 around the c axis.

As we observe six different centers, among which the shallowest could be created even by self-trapping mechanism and other ones have to be stabilized by defects of different origin, high similarity of their g-factor sequence indicates that the largest axial component of the crystal field is produced by Al-O-Al… chains as in the undistorted perovskite lattice. For the $2p_\pi$ ground state the g factors can be described by the following expressions previously introduced for the O_2^- molecule in alkali halides,[31] which has the same p_π ground state:

$$g_1 = g_e \cos\,\vartheta - l\left(\frac{\lambda}{D}\right)(\cos\,\vartheta + 1 - \sin\,\vartheta), \tag{1a}$$

$$g_2 = g_e \cos\,\vartheta - l\left(\frac{\lambda}{D}\right)(\cos\,\vartheta - 1 + \sin\,\vartheta), \tag{1b}$$

$$g_3 = g_e + 2l \sin\,\vartheta \tag{1c}$$

with $\sin\,\vartheta = \lambda/2E$ and $g_e = 2.0023$. Here D is the distance to the highest p_σ orbital in the hole representation, E is the splitting of the twofold-degenerate p_π orbital, and l is a correction to the O^- orbital angular momentum. λ is an effective spin-orbit coupling constant of the O^- ion. Its value in a crystal is usually smaller than that of free ion because of covalency. Taking $l=1$ as for the free O^- ion and $\lambda \approx -150$ cm^{-1} (see, e.g., Ref. 32), one can determine, for example, for the O_I^B center the following splitting of $2p$ orbitals: $D=25\,000$ cm^{-1} and $E=5200$ cm^{-1}. Note that the accuracy of the determination of the crystal-field splittings undoubtedly depends on the values of l and λ which both could be somewhat reduced by the covalence effects. However, even allowing some uncertainty in the l and λ values, the calculated energy splitting seems quite reasonable and are in a good agreement with those obtained for similar O^- centers in the other perovskite $BaTiO_3$.[32] The model with the $2p_\pi$ ground state is also in good agreement with electronic-structure calculations for perovskites, where the O $2p_\pi$ states dominate the upper part of the valence band[13] and therefore, an electron can easily leave the p_π orbital. On the other hand, the model with a p_σ ground state used in Ref. 21 leads to an unrealistically high rhombicity of the center, $D \approx 15\,800$ cm^{-1} and $E \approx 10\,900$ cm^{-1}.[21]

Additional information about the structure of O^- centers can be obtained from the hyperfine (HF) splitting of the spectra. As mentioned above, O^- spectra have the same pronounced HF structure originating from the interaction of a hole with two nearly equivalent ^{27}Al nuclei. The HF interaction is stronger for the O_I-type centers because of a shorter O-Al distance along the c axis ($d[O_I\text{-Al}]=1.901$ Å). For an oxygen ion in the Al plane the shortest O-Al distance is larger ($d[O_{II}\text{-Al}]=1.911$ Å). Consequently, the HF constant for the O_{II} site is about 20% smaller. Furthermore, the HF structure suggests that the perturbing defect is surely located at the Y site because two Al ions in the vicinity of O^- remain at their lattice positions for all the centers. We shall discuss the possible origin of these defects in the next paragraphs.

2. *Thermal stability of* O^- *centers*

An important characteristics of any charge trap in a scintillating material is its energy depth because the charge carriers thermally freed from traps can directly contribute to the delayed radiative recombination processes. In order to obtain quantitative characteristics of the thermal stability of the O^- centers we used the method of isochronal annealing. After irradiation at low temperature (about 10 K), the sample was heated to a given temperature T_{an}, held at that temperature for three minutes, and then quickly cooled (with a rate of about 4 K/s) to 50 K (in the case of the O_I^A center to 12 K), where the ESR spectrum was measured. The three-minute interval was found as the best compromise to ensure good thermalization of the sample and sufficient reproducibility in the measured ESR signal intensities. The obtained signal amplitudes are depicted in Fig. 4. It can be seen that the shallow O_I^A, O_{II}^A and O_{II}^B centers appear simultaneously after irradiation at 10 K. As a result of heating these spectra vanish in turn and other spectra appear; i.e., the hole centers are gradually transforming one into another.

In order to get a deeper insight into kinetics of the trapped holes and their contribution to TSL, we performed a calculation of the thermal-ionization energy and the frequency

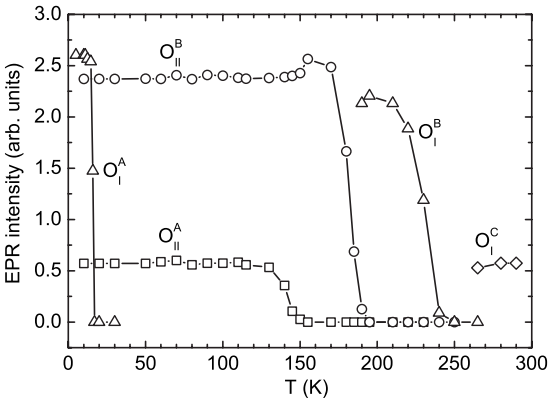

FIG. 4. Dependence of O^- ESR intensities on the temperature of isochronal annealing.

factor using the data of the time decay of ESR intensity measured at constant temperatures. These parameters can be usually obtained from the ionization probability expressed in the form of the Arrhenius law,

$$P(T) = N_c S v \times \exp(-E/kT). \quad (2)$$

Here N_c is an effective density of states in the valence band, v and S are the hole thermal velocity and cross section of its capture, respectively, and E stands for the thermal-ionization energy. The same expression (2) is usually used in the analysis of TSL data. The value of P as a function of temperature can be obtained from the measurements of the time decay $\tau(T)=1/P(T)$ of O^- concentration after turning off the irradiation. As an example, such data are presented in Fig. 5 for one of the centers. One can see that the concentration decay of localized holes approximately obeys the exponential time dependence. Such dependence characterizes a simple first-order kinetic process. The slope of logarithm of the ionization probability as a function of the inverse temperature gives the thermal-ionization energy (see the inset of Fig. 5)

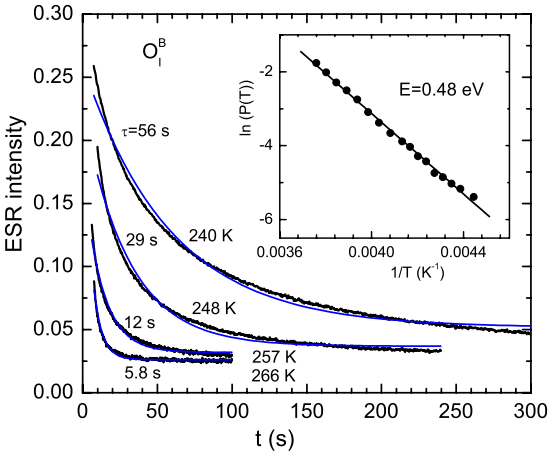

FIG. 5. (Color online) Time decay of the O^- ESR intensity measured at various temperatures. The inset shows the temperature dependence of the thermal-ionization probability of the O_I^B center. Solid lines in both graphs are numerical fits to the data (see the text).

and the frequency factor $s=N_c S v$ can be calculated as well. The ionization energies and frequency factors were determined for the four shallowest hole centers (see Table I). The other hole centers have larger ionization energies and the decay time of their ESR intensity is long even at room temperature. For example, the O_{II}^C center shows a decay time of about 3–5 days. Therefore, the ionization energies of these deep centers could not be determined by ESR method. Now we shall discuss the origin of O^- hole centers in YAP and possible types of perturbing defects.

3. Local structure and creation mechanism

Generally, in perovskite lattice an O^- hole center can be created either by self-trapping mechanism or the hole can be trapped at an oxygen ion located near to a defect. The shallowest O_I^A center can arise due to self-trapping mechanism. This assumption can only partly be supported by the measured ESR data because both unperturbed and perturbed O sites have the same orthorhombic local symmetry. However, the fact that the principal-axis frame of the O_I^A center is turned around the c axis by the angle of 22° with respect to the a axis suggests that the trapped hole is not too strongly coupled to the Y site where a defect could be located. Furthermore, the intensity of the O_I^A spectrum is even higher in the undoped crystal, which was grown from Y_2O_3 oxide of higher 6N purity, with respect to Ce 0.005 at. % doped YAP, where the concentration of accidental impurities must be much higher due to the use of 5N purity Y_2O_3 oxide. Hence the hole self-trapping in the case of O_I^A center is highly probable.

In the case of a defect at the Y site (A_Y) the hole can be trapped at any of the 12 oxygen ions in the neighborhood. There are four O_I-type ions and eight O_{II}-type ions. However, due to different Y-O distances the trapped hole will relax to the most energetically preferable position which should correspond to the shortest A_Y-O distance. Therefore only one of the A_Y-O_I configuration or two equivalent A_Y-O_{II} configurations will be realized for each of the A_Y defect as we observe in the experiment (Table I and Fig. 3).

The three shallowest O^- centers appear simultaneously with approximately the same ratio of concentrations in two crystals of different purity. Therefore, O_{II}^A, O_I^B and O_{II}^B are rather related to intrinsic defects such as Y vacancies and Al_Y antisite ions the concentration of which is expected to be high due to the high-growth temperature and slightly yttrium deficient melt.[25] On the other hand, the intensity of O_I^C and O_{II}^C spectra is about 1 order-of-magnitude lower in the undoped sample of higher purity, clearly indicating the impurity-related origin of these O^- centers.

B. Electron centers

As pointed out above, after x-ray or UV (280–365 nm) irradiation of YAP at $T<77$ K several ESR spectra appear at magnetic fields corresponding to g-factor values less than $g_s=2.0023$ (Fig. 1). This finding suggests that all these spectra belong to the electron-type intrinsic or impurity-related paramagnetic defects. The spectra disappear after the crystal is kept at room temperature for 3–10 days. To identify the

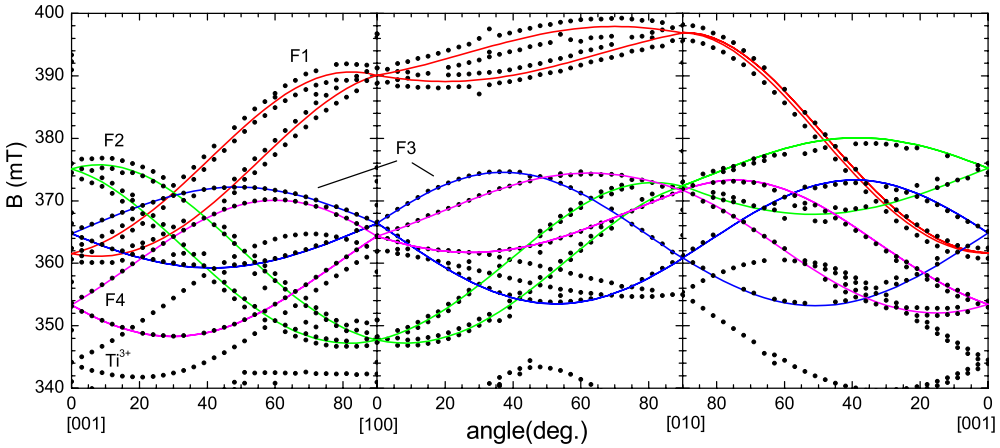

FIG. 6. (Color online) Angular dependencies of resonance fields for electron-type centers in YAP crystal measured at $T=20$ K. Symbols and solid lines are measured and calculated resonance fields, respectively.

origin of the observed defects we carried out measurements of angular dependencies of their resonance lines at three crystallographic planes: (001), (100), and (010). The results are shown in Fig. 6. The spectrum with resonances at lowest magnetic fields has already been assigned to the Ti^{3+} ion.[29] Remaining lines belong to four different centers, denoted F1 to F4, each of them has four magnetically inequivalent positions in the lattice as it follows from the splitting of the resonance lines when the magnetic-field tilts from the cubic ⟨100⟩ directions. The g-factor values suggest that all centers are created by nd^1 ions. The idea is also supported by the short times of their spin-lattice relaxation that allows observing resonances only at $T<30-50$ K. Two of the centers show small (~0.3–0.5 mT) additional splitting of the resonance lines which originates from the interaction of an electron with a single Al nucleus. The simulation of this HF structure is shown in Fig. 7.

The resonance fields were described by the spin Hamiltonian $\mathbf{H}=\mu_B\mathbf{BgS}$ with spin $S=1/2$ and g factors and their principal-axis directions presented in Table II. The g-tensor components are typical for an electron trapped at an nd^1 electronic shell. All four centers have approximately axial symmetry along the g_3 principal direction. For the F1 center the axial axis is oriented close to the direction of O_I-Al-O_I chains. Such a significant axial distortion in the perovskite lattice is usually produced by an oxygen vacancy (V_O). For the F2 center the axial axis lies in the plane of Al ions. Consequently, the axial distortion for the F2 center can be produced by an oxygen vacancy in the O_{II} position. The proposed models of F1 and F2 centers are schematically depicted in Fig. 8. Both centers contain the antisite yttrium ion (Y_{Al}^{2+}) near the oxygen vacancy. It is assumed that an electron, primarily trapped by the oxygen vacancy, is mainly localized at this neighboring Y_{Al} ion. The model of the centers is supported by both the g factors (1.66–1.90) typical for

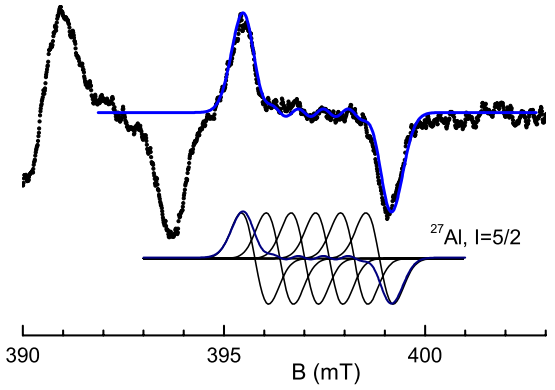

FIG. 7. (Color online) Simulation of the ^{27}Al HF structure of the F1 center at $\angle(B,b)=10°$. The upper part of the figure represents the comparison of the measured spectrum (points) with the simulated one (solid line) taking the Gaussian line shape for the HF lines with the linewidth 0.68 mT and HF splitting 4.8×10^{-4} cm^{-1}. The decomposition of the ^{27}Al HF structure into six individual lines together with their sum is shown at the bottom of the figure too.

TABLE II. Spectral characteristics of electron traps in $YAlO_3$ crystals obtained from the ESR data. Principal-axis directions of g tensors are given by polar (θ) and azimuthal (φ) angles relative to a,b,c-crystal axes and presented for one of four equivalent centers. Error margin of the polar and azimuthal angles is approximately 2°. V_{OI} and V_{OII} correspond to the oxygen vacancy placed in the Y and Al plane, respectively.

Center	g factors	Principal-axis directions θ	Principal-axis directions φ	HF splitting (10^{-4} cm^{-1})
F1:	$g_1=1.6910(4)$	82	21	^{27}Al:
Y_{Al}^{2+}-V_{OI}	$g_2=1.6559(4)$	92	111	$A=4.8(2)$
	$g_3=1.8247(3)$	8	189	
F2:	$g_1=1.7848(4)$	126	107	^{27}Al:
Y_{Al}^{2+}-V_{OII}	$g_2=1.7339(4)$	38	87	$A\approx3.5$
	$g_3=1.9016(4)$	100	10	
F3	$g_1=1.7713(3)$	37	199	Unresolved
	$g_2=1.7576(3)$	73	313	
	$g_3=1.8988(3)$	58	54	
F4	$g_1=1.7833(4)$	124	25	Unresolved
	$g_2=1.7597(4)$	92	116	
	$g_3=1.9015(4)$	34	29	

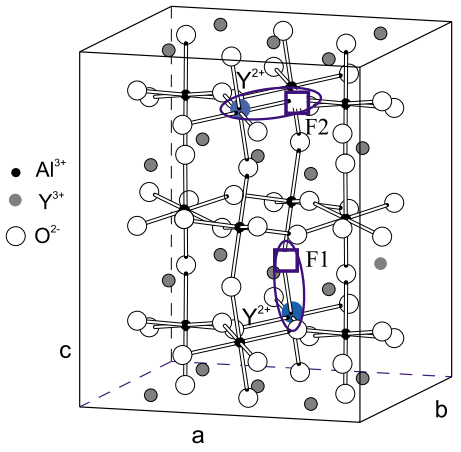

FIG. 8. (Color online) Fragment of YAP crystal structure with the models of Y_{Al}^{2+}-V_O electron centers.

the Y^{2+} $4d^1$ electron configuration (see, e.g., Refs. 33 and 34) as well as the HF interaction of an electron with only one ^{27}Al nucleus since the second Al ion in the Al-V_O-Al chain is replaced by the yttrium antisite ion. Due to shorter V_O-Al distance, ^{27}Al HF interaction, as in the case of O^- centers, is stronger for the oxygen-vacancy sites in the Y planes ($4.8\cdot10^{-4}$ cm^{-1}) with respect to those in the Al planes (3.5×10^{-4} cm^{-1}). HF interaction of an electron with the ^{89}Y isotope ($I=1/2$, natural abundance 100%) should also produce a HF splitting. Such splitting was not resolved in the spectrum presumably due to the small value of the ^{89}Y nuclear magnetic moment (5.3 times smaller than that of ^{27}Al) and partial delocalization of the electron density over the center. The Fermi-contact interaction at the ^{89}Y nuclei can also be partly compensated by the contribution of exchange polarization with an opposite sign. However, the overall reason for small ^{89}Y HF interaction is not completely clear. As mentioned in Sec. I, both oxygen vacancies and antisite ions are the most probable defects in YAP crystals. Our ^{89}Y NMR measurements in fact revealed about 2.5% of Y ions in antisite positions (see Sec. III C). F1 and F2 defects can be thus described as Y_{Al}^{2+}-V_O complexes.

We should note that the ionic radius of Y^{3+} at the Al position (1.04 Å) is markedly larger than that of Al^{3+} (0.675 Å). However, the presence of an oxygen vacancy near the Y_{Al} ion can reduce the ionic radius of Y^{3+} to the value comparable to the ionic radius of Al^{3+} in the regular octahedron due to lowering of the coordination number. The oxygen vacancy also provides more space for location of Y at the octahedral site allowing, in particular, to shift the Y ion toward the oxygen vacancy.

The measured g factors of the electron centers can be easily described by assuming the ground-state wave functions of $T_2(xy)$ type. The expressions for g values of this ground state are completely similar to those previously used in description of the Ti^{3+} spectra in YAP,[29]

$$g_1 = 2 - 2\lambda/\delta_1 + \lambda^2/2\delta_1^2 - \lambda^2/2\delta_2^2 + 2\lambda^2/\delta_2 D,$$

$$g_2 = 2 - 2\lambda/\delta_2 - \lambda^2/2\delta_1^2 + \lambda^2/2\delta_2^2 + 2\lambda^2/\delta_1 D,$$

$$g_3 = 2 - 8\lambda/D - \frac{1}{2}(\lambda/\delta_1 + \lambda/\delta_2)^2 + 2\lambda^2/D^2. \quad (3)$$

Here δ_1 and δ_2 are the energy splitting of the $|zx\rangle$ and $|zy\rangle$ states of the t_{2g} orbital triplet, D is the energy distance to the upper $|x^2-y^2\rangle$ state, and $\lambda\approx300$ cm^{-1} is the effective spin-orbit coupling constant of the Y^{2+} ion.[35] The calculations, for instance, provide the following energy separations: $\delta_1=1680$ cm^{-1}, $\delta_2=1900$ cm^{-1}, and $D=19\,000$ cm^{-1} for the F1 center. Even taking into account some uncertainty of the λ value (it can be, for example, reduced more from the free-ion value), the energy separations seem completely reasonable for the $4d^1$ ion in the perovskite lattice.

Alternatively we can consider an $e_g(d_{3z^2-r^2})$-type ground state for F1/F2 centers. This electronic structure was predicted, for instance, for the single-charged oxygen vacancy in perovskites $BaTiO_3$ and $PbTiO_3$ from *ab initio* calculations.[36] For the $e_g(d_{3z^2-r^2})$ ground state, the crystal-field theory predicts that the g factor measured along the axial distortion has to be close to the $g_e=2.0023$. In principle, taking into account a mixing of $|x^2-y^2\rangle$ orbital to the ground state by orthorhombic components of the crystal field,[37] a covalence contribution from the neighboring shell of yttrium cations[38] and second-order corrections ($\delta g\sim\lambda^2/D^2$), one could justify the large deviation of the largest g factor $g_3=1.8247$ and 1.9016 of the F1 and F2 centers from $g_e=2.0023$ value. However, in this case, the fitting parameters seem to be too unrealistic. Therefore we prefer to model the centers having the ground-state wave functions of $T_2(xy)$ type which adequately (in natural way) describes the experimental g factors. In such a case the unpaired electron resides primarily on the Y^{2+} ion and the oxygen vacancy can be filled even with two electrons. Such scenario is realized, for instance, for Ti^{3+}-V_O centers in $BaTiO_3$.[39] Obviously, a ground state of an oxygen-vacancy-related center is sensitive to the lattice structure and type of transition-metal ion. Calculation in the point-ion crystal-field approximation shows[40] that transition-metal ion—oxygen-vacancy-type defect may have d_{xy}, $d_{zx,zy}$, or d_{z^2} ground state depending on the actual lattice structure, the type of nd^1 ion as well as both the sign and value of this nd^1 ion displacement (see, e.g., Fig. 3 of Ref. 40). Therefore, it seems that the problem of the electronic structure of the oxygen-vacancy-related defects in perovskites is still not completely resolved and needs more investigation. It can be further addressed also by accurate *ab initio* calculations.

The two other centers, F3 and F4, are also nearly axially distorted. No HF splitting is visible for these centers. Therefore their origin is not that clear as in the case of the F1 and F2 centers described above. However, the similarity of g factors and comparable thermal stability of all four defects suggest that the F3 and F4 centers also contain Y_{Al} antisite ion which has trapped an electron. For these centers the trapped electron can be additionally stabilized by a nearby impurity in the yttrium lattice site or by an Al_Y antisite ion.[14] Such an Y^{2+} ion will have similar spectral characteristics to those of the Ti^{3+} ion,[29] except the g-factor values which are smaller for Y^{2+} due to its larger spin-orbit coupling constant.

One can see from Fig. 6 and Table II that this indeed takes place for the F3 and F4 centers.

Possible candidates for the photoinduced electronic centers in YAP could be $Sc^{2+}(3d^1)$, $Zr^{3+}(4d^1)$, $La^{2+}(5d^1)$, $Hf^{3+}(5d^1)$, or even $V^{4+}(3d^1)$, $Nb^{4+}(4d^1)$, and $Ta^{4+}(5d^1)$ ions. However all these ions have large nuclear magnetic moments that would result in a characteristic HF splitting of ESR lines unlike the results of the experiment. In addition, all these ions will create deep, at room temperature very stable, paramagnetic centers such as Ti^{3+} (Ref. 29) or Cr^{3+} (Ref. 41) as their local electronic level has to be situated in the middle of the forbidden gap. Independent chemical analysis of the crystal producer indicates that concentration of all these ions is well below 1 ppm. Therefore, taking into account all above presented arguments, the described electronic-type defects in YAP are assigned by us to Y_{Al} antisite ions which trapped an electron under irradiation. Nevertheless, the ^{89}Y HF splitting in the spectra was not resolved. An electron trapped by an Y_{Al} ion can be additionally stabilized either by an oxygen vacancy, creating Y_{Al}^{2+}-V_O centers, or by a defect at the Y site.

C. Evidence about antisite ions from NMR

Recently the antisite defects and related traps in $YAlO_3$ and $LuAlO_3$ were theoretically considered using density-functional theory calculations.[14] These *ab initio* calculations have shown that (i) single antisites in which either an Al ion is placed at the Y(Lu) site or an Y(Lu) ion is placed at the Al site both have low energy with respect to the antisite pair [interchange of neighboring Y(Lu) and Al atoms]; (ii) defects containing Al ion at the Y(Lu) site produce electron traps at 0.4–0.8 eV below the conduction-band edge while Y(Lu) ions on the Al site probably do not. Our results are in good agreement with the first prediction as we did not find any indication on the presence of the Y_{Al}-Al_Y antisite pairs. On the other hand, the electron traps revealed by us include Y_{Al} single antisites. It should also be noted that we do not observe ESR spectra which could be assigned to Al_Y electron traps. Such an antisite ion after trapping an electron becomes a paramagnetic $Al_Y^{2+}(3s^1)$ center. Its spectrum has to be easily visible as the center possesses an electron spin 1/2 and a strong ^{27}Al HF structure is expected too.

In order to clarify the situation with antisite ions in YAP crystals we performed ^{89}Y and ^{27}Al NMR measurements. It is well known that NMR provides unique approach to quantify the site occupancy in crystalline, amorphous, or liquid materials.[42] The NMR signal in a properly designed experiment is directly proportional to the concentration of atoms in a given structural environment. ^{89}Y is a highly suitable isotope as it possesses nuclear spin 1/2. However, due to its small gyromagnetic ratio and long spin-lattice relaxation time (up to 45–60 min) the NMR signal intensity is usually very weak. Nevertheless, accumulation of the signal for 60 h provided a well-resolved ^{89}Y NMR signal from Y antisite positions (Fig. 9). The relative concentration of Y antisite ions was determined as $(2.5 \pm 0.2)\%$. This is the first direct evidence about the existence of Y antisite ions in YAP single crystals. ^{27}Al NMR measurements were also performed. Yet, due to the high nuclear spin of the ^{27}Al isotope ($I=5/2$) to interpret the measured spectra is not as easy as in the case of the ^{89}Y isotope. Therefore, at the present stage the NMR data can neither prove nor disprove the existence of Al_Y antisites in YAP.

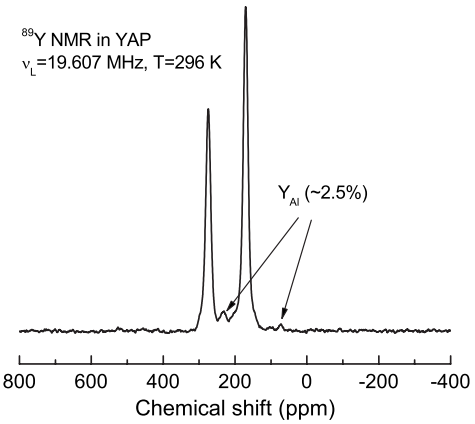

FIG. 9. ^{89}Y NMR spectrum in YAP measured at B II [110] and $T=296$ K. Two strong lines correspond to resonances from regular Y ions while two other weak lines correspond to Y in antisite positions.

D. Electron-hole recombination mechanisms and the role of irradiation-induced defects in scintillation mechanism in YAP:Ce

In our previous papers we provided qualitative correlation between ESR intensity of O^- centers and TSL peaks in undoped YAP crystals (see, e.g., Fig. 6 of Ref. 23). TSL emission spectra of undoped YAP (Ref. 22) suggest that the recombination of thermally liberated holes takes place at intrinsic defects which are assumed to be electron-type F/F^+ centers created by electrons trapped at oxygen vacancies near Y antisite ion. Present ESR data provide further support for this assumption. Hole recombination at Y_{Al}^{2+} ions including the Y_{Al}^{2+}-V_O centers is directly visible from the measured temperature dependence of their concentration under pulsed heating of the irradiated crystal as shown in Fig. 10. One can see that thermal disintegration of each hole center, i.e., diminishing of its ESR intensity, is accompanied by the decrease in the Y_{Al}^{2+} center's related ESR intensity which proves recombination of liberated holes with electrons localized at these centers.

As mentioned in Sec. I, a critical requirement for any fast scintillator is the fast delivery of electrons and holes from the conduction and valence bands, respectively, toward the emission centers, i.e., Ce^{3+} in the case of YAP:Ce. It is generally accepted that Ce^{3+} is an efficient hole trap in YAP host. Therefore migrating holes must be first trapped at Ce^{3+} ions. Subsequent recombination with electrons from the conduction band then provides the desired fast scintillation light. Retrapping of electrons in relatively deep Y_{Al}^{2+} centers can give rise to induced absorption phenomena, i.e., radiation damage of the material[18] since at room temperature these centers can survive for several days. As these localized electrons are lost for prompt radiative recombination at Ce centers some light-yield reduction can also be expected. The

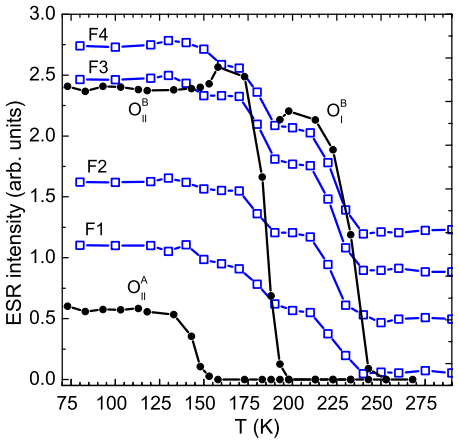

FIG. 10. (Color online) Correlation between ESR intensity of electron Y^{2+}_{Al} centers (empty squares) and thermal destruction of different O^- hole centers (solid circles) showing recombination of liberated holes at Y^{2+}_{Al} centers.

described hole traps compete with the Ce^{3+} centers to capture a hole. Though the YAP lattice provides several possibilities for the creation of intrinsic or impurity-related hole traps, the relatively high concentration of Ce^{3+} in practical YAP:Ce scintillator material (about 0.5 at. % of Ce in the crystal) ensures its success in the competition for hole capture with all the defect-based hole traps. This is supported by the fact that in heavily Ce-doped YAP the O^- concentration is strongly diminished. However, contribution to slower scintillation decay components may appear from the shallowest hole trap as it arises most probably by the self-trapping mechanism. Fortunately, the thermal stability of the self-trapped hole in YAP lattice is even smaller than in the very efficient Lu_2SiO_5:Ce scintillator.[43] Therefore probably no significant delay in radiative recombination at Ce^{3+} centers should be expected due to this YAP-lattice property.

IV. CONCLUSIONS

Trapping phenomena and the nature of trapping sites in pure and slightly Ce-doped YAP crystals were investigated by the ESR method. In addition to two already known O^- hole centers[21] four other O^- centers were identified and studied. These centers are created by trapping holes from the valence band by oxygen anions under UV or x-ray irradiation at low temperature. The centers differ by their thermal stability and spectral parameters. With increasing temperature they are progressively transforming one into another. Our analysis has shown that the shallowest O^- hole center (thermal activation energy E_a=0.024 eV) is most probably created by a self-trapping mechanism. Three other O^- centers, denoted as O^A_{II}, O^B_I, and O^B_{II}, are stabilized by intrinsic defects such as Y vacancies and possibly Al_Y antisite ions, which stabilize a hole at a nearby oxygen ion. The thermal stability of these centers is described by activation energies of 0.40, 0.49, and 0.48 eV, respectively. The two deepest hole centers, O^C_I and O^C_{II}, are stable even at room temperatures for a few days. The holes are stabilized here by an impurity ion at the Y site. The thermally induced decay of the four shallowest O^- centers is accompanied by well-resolved TSL peaks below room temperature. This means that when a hole is liberated from an O^- center, it is either captured at a deeper hole trap or it migrates until a localized electron is met. The resulting electron-hole pair radiatively recombines which gives rise to a TSL glow peak.

Electronic-type trapping sites are assigned to the yttrium antisite ions which become paramagnetic Y^{2+}_{Al} centers after trapping an electron. They are found in four structurally different configurations with a thermal stability around or higher than 300 K that enables the radiative recombination of thermally liberated holes with such localized electrons. In two of the centers, F1 and F2, the trapped electron is additionally stabilized by an oxygen vacancy. These centers can be described as Y^{2+}_{Al}-V_{OI} and Y^{2+}_{Al}-V_{OII} complexes, where O_I and O_{II} correspond to the oxygen ions in the Y and Al planes, respectively. Two other centers are created by yttrium antisite ions nearby a defect at Y site.

Yttrium antisite positions in YAP lattice were directly identified by ^{89}Y nuclear magnetic-resonance measurements. On the other hand, our work did not confirm the existence of Al^{2+}_Y paramagnetic centers associated with Al_Y antisite ions the existence of which is also considered in the literature.

ACKNOWLEDGMENTS

The authors gratefully acknowledge the financial support of the Czech Project (Project No. GA AV IAA100100810) and the Institutional Research Plan (Plan No. AVOZ10100521). The financial support of the CARIPLO Foundation project "Energy transfer and trapping processes in nanostructured scintillator materials" (2008–2011) is also gratefully acknowledged.

[1] *Heavy Scintillators for Scientific and Industrial Applications: Proceedings of the Cristal 2000 International Workshop*, Chamonix, France, 1992, edited by F. de Notaristefani, P. Lecoq, and M. Schneegans (Editions Frontieres, Gif-sur-Yvette, France, 1993), pp. 1–152.

[2] T. Takeda, T. Miyata, F. Muramatsu, and T. Tomiki, J. Electrochem. Soc. **127**, 438 (1980).

[3] I. A. Kamenskikh, N. Guerassimova, C. Dujardin, N. Garnier, G. Ledoux, C. Pédrini, M. Kirm, A. Petrosyan, and D. Spassky, Opt. Mater. **24**, 267 (2003).

[4] M. Nikl, N. Solovieva, J. Pejchal, J. B. Shim, A. Yoshikawa, T. Fukuda, A. Vedda, M. Martini, and D. H. Yoon, Appl. Phys. Lett. **84**, 882 (2004).

[5] C. Pedrini, D. Bouttet, C. Dujardin, B. Moine, I. Dafinei, P. Lecoq, M. Koselja, and K. Blazek, Opt. Mater. **3**, 81 (1994).

[6] M. Zhuravleva, A. Novoselov, E. Mihokova, J. A. Mares, A.

Vedda, M. Nikl, and A. Yoshikawa, IEEE Trans. Nucl. Sci. **55**, 1476 (2008).
[7] Yu. V. Zorenko, M. V. Pashkovsky, M. M. Batenchuk, L. M. Lymarenko, and I. V. Nazar, Opt. Spectrosc. **80**, 776 (1996).
[8] M. M. Kuklja, J. Phys.: Condens. Matter **12**, 2953 (2000).
[9] C. W. E. van Eijk, Nucl. Instrum. Methods Phys. Res. A **460**, 1 (2001).
[10] A. Vedda, M. Martini, F. Meinardi, J. Chval, M. Dusek, J. A. Mares, E. Mihokova, and M. Nikl, Phys. Rev. B **61**, 8081 (2000).
[11] V. V. Laguta, M. Martini, A. Vedda, M. Nikl, E. Mihóková, P. Boháček, J. Rosa, A. Hofstätter, B. K. Meyer, and Y. Usuki, Phys. Rev. B **64**, 165102 (2001).
[12] C. R. Stanek, K. J. McClellan, M. R. Levy, and R. W. Grimes, J. Appl. Phys. **99**, 113518 (2006).
[13] W. Y. Ching and Y.-N. Xu, Phys. Rev. B **59**, 12815 (1999).
[14] D. J. Singh, Phys. Rev. B **76**, 214115 (2007).
[15] V. Babin, P. Fabeni, A. Krasnikov, K. Nejezchleb, M. Nikl, G. P. Pazzi, T. Savikhina, and S. Zazubovich, J. Lumin. **124**, 273 (2007).
[16] M. Nikl, J. A. Mares, J. Chval, E. Mihokova, N. Solovieva, M. Martini, A. Vedda, K. Blazek, P. Maly, K. Nejezchleb, P. Fabeni, G. P. Pazzi, V. Babin, K. Kalder, A. Krasnikov, S. Zazubovich, and C. D'Ambrosio, Nucl. Instrum. Methods Phys. Res. A **486**, 250 (2002).
[17] Y. Zorenko, V. Gorbenko, I. Konstankevych, T. Voznjak, V. Savchyn, M. Nikl, J. A. Mares, K. Nejezchleb, V. Mikhailin, and V. Kolobanov, Radiat. Meas. **42**, 528 (2007).
[18] J. A. Mares, M. Nikl, E. Mihokova, N. Solovieva, K. Blazek, K. Nejezchleb, P. Maly, J. Pejchal, V. Mucka, M. Pospisil, A. Vedda, M. Martini, and S. Baccaro, Radiat. Eff. Defects Solids **157**, 677 (2002).
[19] A. J. Wojtowicz, J. Glodo, W. Drozdowski, and K. R. Przegietka, J. Lumin. **79**, 275 (1998); A. J. Wojtowicz, J. Glodo, A. Lempicki, and C. Brecher, J. Phys.: Condens. Matter **10**, 8401 (1998).
[20] J. B. Shim, A. Yoshikawa, M. Nikl, J. Pejchal, A. Vedda, and T. Fukuda, Radiat. Meas. **38**, 493 (2004).
[21] O. F. Schirmer, K. W. Blazey, and W. Berlinger, Phys. Rev. B **11**, 4201 (1975).
[22] M. Nikl, V. V. Laguta, and A. Vedda, Phys. Status Solidi A **204**, 683 (2007).
[23] M. Nikl, V. V. Laguta, and A. Vedda, Phys. Status Solidi B **245**, 1701 (2008).
[24] M. Fasoli, I. Fontana, F. Moretti, A. Vedda, M. Nikl, E. Mihokova, Yu. V. Zorenko, and V. I. Gorbenko, IEEE Trans. Nucl. Sci. **55**, 1114 (2008).
[25] J. Kvapil, B. Manek, B. Perner, J. Kvapil, R. Becker, and G. Ringel, Cryst. Res. Technol. **23**, 549 (1988).
[26] S. Geller and E. A. Wood, Acta Crystallogr. **9**, 563 (1956); R. Diehl and G. Brandt, Mater. Res. Bull. **10**, 85 (1975).
[27] A. Vedda, M. Fasoli, M. Nikl, V. V. Laguta, E. Mihokova, J. Pejchal, A. Yoshikawa, and M. Zhuravleva, preceding paper, Phys. Rev. B **80**, 045113 (2009).
[28] V. V. Laguta, A. M. Slipenyuk, J. Rosa, M. Nikl, A. Vedda, K. Nejezchleb, and K. Blazek, Radiat. Meas. **38**, 735 (2004).
[29] M. Yamaga, T. Yosida, B. Henderson, K. P. O'Donnell, and M. Date, J. Phys.: Condens. Matter **4**, 7285 (1992).
[30] S. A. Basun, T. Danger, A. A. Kaplyanskii, D. S. McClure, K. Petermann, and W. C. Wong, Phys. Rev. B **54**, 6141 (1996).
[31] H. R. Zeller and W. Känzig, Helv. Phys. Acta **40**, 845 (1967); W. Känzig and M. H. Cohen, Phys. Rev. Lett. **3**, 509 (1959).
[32] T. Varnhorst, O. F. Schirmer, H. Kröse, R. Scharfschwerdt, and Th. W. Kool, Phys. Rev. B **53**, 116 (1996).
[33] J. R. Herrington, T. L. Estle, and L. A. Boatner, Phys. Rev. B **7**, 3003 (1973).
[34] H. Bill, G. Magne, C. Balesta, and D. Lovy, J. Phys. C **19**, L19 (1986).
[35] T. M. Dunn, Trans. Faraday Soc. **57**, 1441 (1961); M. Blume, A. J. Freeman, and R. E. Watson, Phys. Rev. **134**, A320 (1964).
[36] H. Donnerberg and A. Birkholz, J. Phys.: Condens. Matter **12**, 8239 (2000); H. Pinto, S. Elliott, and A. Stashans, Proc. SPIE **5122**, 303 (2003).
[37] Z. Šroubek and K. Ždánský, J. Chem. Phys. **44**, 3078 (1966).
[38] A. Hofstätter, A. Scharmann, D. Schwabe, and B. Vitt, Z. Phys. B **30**, 305 (1978).
[39] S. Lenjer, O. F. Schirmer, H. Hesse, and Th. W. Kool, Phys. Rev. B **66**, 165106 (2002).
[40] V. V. Laguta, M. D. Glinchuk, R. O. Kuzian, S. N. Nokhrin, I. P. Bykov, L. Jastrabik, and J. Rosa, Solid State Commun. **122**, 277 (2002).
[41] M. Yamaga, H. Takeuchi, T. P. J. Han, and B. Henderson, J. Phys.: Condens. Matter **5**, 8097 (1993).
[42] A. Abragam, *The Principles of Nuclear Magnetism* (Oxford University Press, New York, 1961).
[43] D. W. Cooke, B. L. Bennett, R. E. Muenchausen, J.-K. Lee, and M. A. Nastasi, J. Lumin. **106**, 125 (2004).